Variability of lightning hazard over Indian region with respect to ENSO Phases

Avaronthan Veettil Sreenath[1], Sukumarapillai Abhilash[1,2], and Pattathil Vijaykumar[1,2]

[1]Department of Atmospheric Sciences, Cochin University of Science and Technology, Cochin 682016, India
[2]Advanced Department Centre for Atmospheric Radar Research, Cochin University of Science and Technology, Cochin 682022, India

Correspondence: S Abhilash (abhimets@gmail.com)

Abstract.

The El-Nino Southern Oscillation (ENSO) modulates the ~~lightning flash rate (LFR~~Lightning Flash Density (LFD) variability over India during pre-monsoon, monsoon, and post-monsoon seasons. This study intends to shed light on the impact of ENSO phases on the ~~LFR~~ LFD over the Indian subcontinent using the data obtained from Optical Transient Detector (OTD) and Lightning Imaging Sensors (LIS) onboard the TRMM satellite. Results suggest ~~that irrespective of ENSO phases, the LFR is maximum over northeast India (NEI) in the pre-monsoon season, and the peak is shifted to the north of northwest India (NNWI) in the monsoon season. The LFR~~ the LFD over Northeast India (NEI) and southern peninsular India (SPI) strengthened (weakened) during the warm (cold) phase of ENSO in the pre-monsoon season. During monsoon season, ~~NEI (NNWI~~ NNWI (north of northwest India) shows above ~~normal LFR in the warm (cold~~ (below) normal LFD in the cold (warm) ENSO phase. It is striking to note that ~~the~~ there are three hotspots of ~~LFR~~ LFD over the Indian land region, which became more prominent ~~in the last decade of the monsoon season~~during the monsoon seasons of the last decade. A widespread increase of ~~LFR~~ LFD is observed all over India during the warm phase of ENSO in the post-monsoon season. A robust rise in graupel/snow concentration is found during the post-monsoon season over SPI in the ENSO phase, with the lowest fluctuations over the NEI and NNWI regions. The subtropical westerly jet stream is shifted south in association with the warm phase, ~~with an associated increase in the~~ accompanied by an increase of geopotential height (GPH) all over India ~~in~~ for the same period. This exciting remark ~~might~~ may explain the indirect influences of ENSO~~'~~'s warm phase on ~~LFR~~ LFD during the post-monsoon season by pushing the mean position of subtropical westerly towards ~~south~~ southern latitudes. However, the marked increase of ~~LFR~~ LFD is confined mostly over the NNWI in the cold ENSO phase.

1 Introduction

Lightning is a tremendous and inescapable atmospheric hazard that humankind has encountered throughout history (Cooray et al., 2007; Mills et al., 2010). The number of casualties underlines lightning hazards as a devastating phenomenon, with an annual death rate of 2234 from 2001 to 2014 over India (Selvi and Rajapandian, 2016). Singh and Singh (2015) documented the yearly number of lightning fatalities and lightning flashes in India from 1998 to 2005, and they find that the fatalities increase coherently with the lightning flash rate. Lightning strikes over the plain terrains are observed to be less as compared to the hilly

25 regions. Due to the former's high population density, even lesser lightning flashes take many people's lives due to high chances of being struck by lightning (Yadava et al., 2020).

The El-Nino Southern Oscillation (ENSO) is a naturally occurring planetary-scale phenomenon related to the variations in sea surface temperatures over the tropical Pacific Ocean, strongly influencing the number of flashes and average flash rate (Kumar and Kamra, 2012). It is one of the most dynamic climatic variability modes, characterized by three phases: El-Nino

30 (Warm), La-Nina (Cold), and Neutral. The ENSO is a crucial player in the transport of heat, moisture, and momentum and modulates the frequency, intensity, and location of deep convection and the associated lightning activity (Williams, 1992; Kulkarni and Siingh, 2014). Higher Lightning Flash ~~Rate (LFR~~Density (LFD) areas are located away from the equator during the warm phase and coincide with regions of anomalous jet stream circulation enhanced by the meridional heat transport (Chronis et al., 2008). Kandalgaonkar et al. (2010) has reported that lightning activity during the El-Nino year of 2002 increased

35 by 18% over the Indian land region compared to the La-Nina years during 1998-2011. On a global scale, lightning activity shows strong regional preference during different ENSO Phases.

The changes in the lower and upper air circulations associated with different ENSO phases have been found to influence the storm frequency and intensity (Yang et al., 2002; Hsu and Wallace, 1976), which in turn affect the lightning activity (Goodman et al., 2000). Kent et al. (1995) observed that ENSO could dictate clouds' distribution over the tropics and subtropics. Owing

40 to the presence of anomalous subsidence over the western Pacific and adjacent landmass, deep convective clouds are inhibited; hence the rainfall is less during the warm phase (Cess et al., 2001). A southward/eastward shift in the global lightning activity is visible during the warm phase, and the latitudes corresponding to the descending limb of the Hadley circulation exhibit the most significant contrast of ~~LFR~~ LFD between the warm and cold phase of the ENSO (Sátori et al., 2009).

Generally, lightning activity is ~~controlled~~ tuned by the clouds growing deep into the atmosphere. The deep convective

45 cores present over India's east coast during the pre-monsoon season shift to the foothills of western Himalayas during the monsoon (Romatschke et al., 2010). Cecil et al. (2014) documented that India's offshore regions and the maritime continent are prone to deep convection. The vertical growth of cloud systems is amplified by the intense updraft, promoting ice crystals and supercooled liquid (mixed-phase) inside the convective system. The interaction between these hydrometeors is mainly responsible for the electrification inside the cloud (Takahashi et al., 1999; Williams, 2001). The atmosphere's dynamic and

50 thermodynamic states also modulate the lightning activity over a region (Williams, 1992; Zipser, 1994; Petersen et al., 1996; Rosenfeld, 1999). Topography is ~~also identified as a~~ identified as another critical participant in developing deep convective clouds and impacts the distribution of lightning activity (Kilinc and Beringer, 2007). Earlier studies have observed that elevated landmass favours the development of deep convective clouds (Zipser et al., 2006; Houze Jr et al., 2007; Rasmussen and Houze Jr, 2011) and thereby leading to higher ~~LFR. Another agent that plays~~ LFD. In addition, aerosols are also considered

55 a contributor for making a decisive role in generating lightning ~~activity is aerosols~~flashes. Higher aerosol loading increases the available liquid water in the mixed-phase condition, ~~which is~~ an essential factor for cloud electrification and lightning activity (Williams et al., 2002). Venevsky (2014) reported a significant correlation between lightning and concentration of annually-averaged cloud condensation nuclei over both land and ocean.

The awareness of lightning safety among the public is relatively low. The present study ~~provides vital information~~ aims to provide vital information to the public on the risky lightning periods over the Indian subcontinent and how the large scale phenomenon, ENSO, is influencing the same. We are detailing the modulation of ~~LFR~~ LFD under different ENSO phases with the help of a vertical profile of hydrometeors (graupel and snow) inside the cloud systems and related atmospheric dynamics during pre-monsoon (March-May) monsoon (June-September) and post-monsoon (October-December) seasons in India. The ~~variability of LFR and hydrometeor distribution inside the convective system with different ENSO phases are very rare in the literature.~~

~~The organization of this paper is~~ rest of the paper is organized as follows. ~~The datasets~~ Section 2 provides descriptions of the data and methodology employed in this study ~~are described in section 2. In section~~. Section 3 ~~, we present~~ presents the results followed by subsection 3.1, which depicts the composite analysis of ~~LFR~~ LFD for pre-monsoon, monsoon, and post-monsoon seasons corresponding to the three ENSO phases. The remaining subsections of section 3 (3.2, 3.3 and 3.4) portray the composite analysis of anomalous ~~LFR~~ LFD during the different seasons and the significance of vertical cloud structure and associated dynamics in regulating their distribution. Finally, the conclusions of this work are given in section 4.

2 Data and methods

The Lightning Imaging Sensor (LIS) was an instrument onboard the Tropical Rainfall Measuring Mission (TRMM) satellite launched in December 1997. This instrument senses lightning flashes across the global tropics and subtropics (Goodman et al., 2007). The Optical Transient Detector (OTD) was the predecessor of LIS, launched in the MicroLab-1 satellite. Combined OTD (Optical Transient Detector) + LIS (Lightning Imaging Sensor) monthly averaged flash ~~rates expressed flash km-2day-1~~ density expressed flash $km^{-2}.day^{-1}$ available from http://ghrc.nsstc.nasa.gov/ is used in this work. These products compute mean ~~lightning flash rates~~ LFD by accumulating the total number of flashes observed and the entire observation duration for each grid box ($2.5° \times 2.5°$) from the thousands of individual satellite orbits. The lightning climatology derived from OTD / LIS (Cecil et al., 2014) provides a unique observational basis for the global flash distribution in monthly time series (Kamra and Athira, 2016), seasonal cycles (Christian et al., 2003), or diurnal cycles (Blakeslee et al., 2014). To produce the low-resolution monthly time series (~~LMRTS~~LRMTS) data, LIS and OTD flash ~~rates~~ density and view times are smoothed precisely and are extracted for the middle day of each month (Cecil et al., 2014). The ~~lightning flash rates~~ LFD in an LRMTS have slightly over three months of temporal smoothing and $7.5° \times 7.5°$ spatial smoothing (Cecil et al., 2014). The data sets are described in greater detail in the following paper: Gridded lightning climatology from TRMM-LIS and OTD: Dataset description by Cecil et al. (2014).

The ~~LFR~~ LFD data is available starting from July 1995 only. So the pre-monsoon season in our work starts in 1996 (March-May) and ends in 2013 (March-May). Due to data unavailability, the first monsoon season includes only three months (July, August, and September 1995). This particular season terminates in 2013 (June, July, August, and September). On the other hand, the post-monsoon season is prepared from 1995 (October-December) to 2013 (October-December). ~~LFR~~ LFD anomaly in this study indicates the difference between the composite of ~~LFR~~ LFD during a particular ENSO phase in a specific season

and the composite of ~~LFR~~ LFD during all the three ENSO phases in that specific season. e.g., ~~LFR~~ LFD anomaly during pre-monsoon during La-Nina = (Composite of ~~LFR~~ LFD during La-Nina in pre-monsoon) - (Composite of ~~LFR~~ LFD during all the three ENSO phases in pre-monsoon). The anomalies of all other parameters used in this study are calculated using the
95   same method.

With the aid of TRMM-3A12 data, the cloud structure is examined by evaluating the vertical profiles of hydrometeors (graupel, snow~~, rainwater~~) and latent heat release during different phases of ENSO. The data set has a spatial resolution of $0.5° \times 0.5°$, ~~and it is~~ available from January 1998 to December 2013. It has 28 vertical levels, which start from 0.5 km, and each level is separated by 0.5 km. These parameters are averaged for the pre-monsoon, monsoon and post-monsoon season
100   from 1998 to 2013 with respect to La-Nina, El-Nino and Neutral phases of ENSO over northeast India (NEI: 85° E-95° E, 20° N-30° N), north of northwest India (NNWI: 25° N-40° N, 65° E-80° E) and southern peninsular India (SPI: 5° N-15° N, 75° E-80° E) and used in this work.

Finally, the modulation of Geopotential height (GPH) at 500 hPa, wind at 200 hPa, and specific humidity (SH) at 300 hPa are also examined with the ENSO phases from July 1995 to December 2013. The above parameters are obtained from the
105   NCEP–National Center for Atmospheric Research (NCAR) reanalysis data with a similar spatial and temporal resolution of ~~LFR~~ LFD. Oceanic Nino Index (ONI) is the standard used to identify different phases of ENSO. The average value of ONI is determined during pre-monsoon, monsoon, and post-monsoon season by using HadISST data and detailed in table 1. If the ONI value is above (below) $+0.5°$ ($-0.5°$) C, it is taken as the warm (cold) phase, and the neutral phase corresponds to the ONI index lies between $-0.5/+0.5°$ C.

110   ## 3   Results and discussion

3.1   Composite ~~LFR~~ LFD with respect to ENSO phases

Figure 1 represents the ~~LFR~~ LFD composites for pre-monsoon, monsoon, and post-monsoon seasons corresponding to the three ENSO phases. Irrespective of ENSO phases, the ~~LFR~~ LFD peak is located over ~~northeast India (NEI)~~ NEI during the pre-monsoon season, while its peak shifts to the ~~north of northwest India (NNWI)~~ NNWI in the monsoon season. Kamra and
115   Athira (2016) ~~have previously reported a similar type of swing in LFR between~~ identified a higher concentration of LFD over northwest and northeast regions of India, and it is tightly correlated with CAPE over those regions. They also observed that the maxima of lightning during post-monsoon is also lying over India's southern and eastern regions. Ahmad and Ghosh (2017) reported that compared to other Indian regions, lightning activity is higher over the North-Eastern part and southern part of India during the pre-monsoon ~~and monsoon seasons~~ season. Similarly, we have identified three hot spots of higher lightning
120   activity over the Indian subcontinent (Figure 1 (a)). They are located in the NEI (85°E-95°E, 20°N-30°N), NNWI (25°N-40°N, 65°E-80°E) and SPI (5°N-15°N, 75°E-80°E). The Himalayan orography favours the formation of deep convective systems over the NEI (Goswami et al., 2010) and is evidenced by the high values of ~~LFR~~ LFD over the region. Rather than the altitude, the steep topographic gradient is responsible for producing deep convection. Most likely, the deep convective clouds developed in the conditionally unstable atmosphere during the pre-monsoon season are electrically more active (Williams et al., 1992).

Year	Pre-monsoon	Monsoon	Post-monsoon
1995	0.39	-0.08	*-0.60*
1996	-0.27	-0.10	-0.25
1997	**0.51**	**1.81**	**2.41**
1998	**1.15**	*-0.57*	*-1.20*
1999	*-0.73*	*-0.77*	*-1.24*
2000	*-0.80*	-0.39	*-0.65*
2001	-0.22	0.01	-0.25
2002	0.27	**0.81**	**1.40**
2003	0.10	0.15	0.46
2004	0.14	**0.58**	**0.76**
2005	0.41	0.14	-0.36
2006	-0.27	0.39	**1.02**
2007	-0.10	-0.40	*-1.40*
2008	*-0.76*	-0.08	-0.43
2009	-0.35	**0.73**	**1.49**
2010	**0.62**	*-0.97*	*-1.52*
2011	*-0.61*	-0.34	*-0.96*
2012	-0.17	**0.53**	0.21
2013	-0.03	0.39	**0.79**

Table 1. ONI during the pre-monsoon, monsoon, and post-monsoon season in India from 1995 to 2013. The bold, italics and underlined values denote El-Nino, La-Nina, and Neutral phases of ENSO, respectively.

Lau et al. (2008) proposed that during the pre-monsoon months, dust and black carbon from neighbouring sources accumulates over the Indo-Gangetic plain against the foothills of the Himalayas and act as an elevated heat pump (EHP). Accordingly, this enhanced warming of the middle and upper troposphere contributes to the genesis of deep clouds and higher ~~LFR~~LFD.

Compared to monsoon and post-monsoon seasons, convective available potential energy (CAPE) is higher during the pre-monsoon season. The seasonal average of CAPE is highest over India's east coast, and it is near 1500 J/kg all over south India (Murugavel et al., 2014). Nevertheless, large regions of India, especially the central Indian region, show a seasonal average of CAPE less than 1000 J/Kg (Murugavel et al., 2014). Strikingly, the areas of higher values of ~~LFR~~ LFD (Figure 1) during the pre-monsoon season coincide with the regions of CAPE maxima reported by (Murugavel et al., 2014). Previous works ascertain that the moderate updrafts limit the vertical development of convective clouds during the summer monsoon under the influence of maritime air mass (Kumar et al., 2014; Tinmaker et al., 2015), which leads to a decline in the cloud electrification during the monsoon season. Among the three seasons, post-monsoon shows a minimum of ~~LFR~~ LFD over the Indian region (Figure 1)~~, and the NW to the NE gradient of LFR is also observed to be weak in this season~~. One possible reason for this
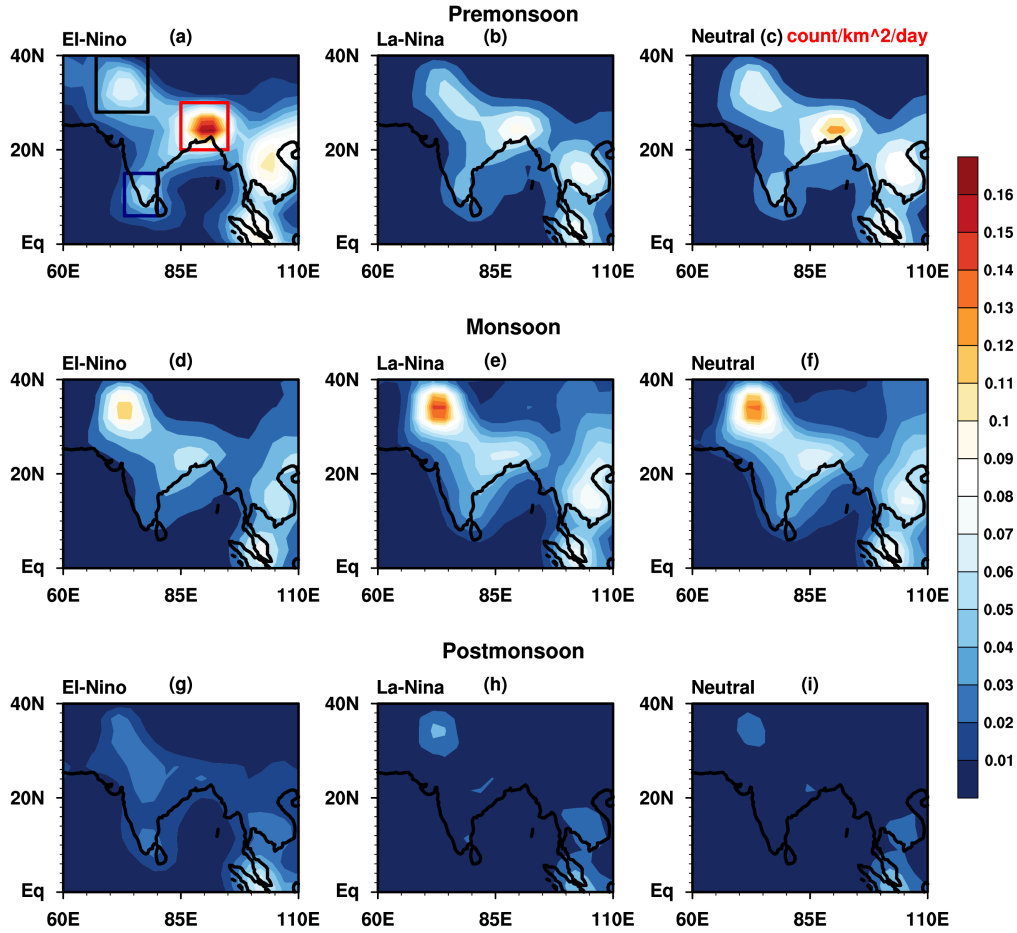
Figure 1. ~~LFR~~ LFD composite during different ENSO phases. Coloured boxes in figure 1 a represents the hotspot regions of LFD (red box = NEI, black box = NNWI, blue box = SPI)

~~is~~ may be the existence of a low average value of CAPE (<500 J/kg) over most parts of India during this season (Murugavel et al., 2014), which is relatively low to favour the development of deep convection and hence lightning.

3.2 ~~Distribution of anomalous LFR during pre-monsoon season with respect to ENSO phases~~

140 ~~Ahmad and Ghosh (2017) reported that compared to other Indian regions, lightning activity is higher over the North-Eastern part and southern part of India during the pre-monsoon season. They also observed that the maxima of lightning during~~ The relationship between LFD and graupel concentration is examined during the three seasons by using a Pearson correlation

analysis over NEI, NNWI and SPI (Figure 2). It shows that the correlation between LFD and graupel concentration is peaking during the post-monsoon ~~is also lying over India's southern and eastern regions. Kamra and Athira (2016) identified a higher~~

145 ~~concentration of LFR over northwest and northeast regions of India, and it is tightly correlated with CAPE over those regions. Similarly, we have identified three hot spots of higher lightning activity over the Indian subcontinent (Figure 1). They are located in the NEI (85°E-95°E, 20°N-30°N~~ season over NEI (r=0.81), NNWI (r=0.64) and SPI (r=0.62). In contrast, the correlation attained a minimum value during the monsoon season over these hotspots regions of LFD (NEI (r=0.24), NNWI (r=0.36), SPI (r=0.38)). It is important to note that the pre-monsoon season also exhibits solid correlation between LFD and

150 graupel concentration over NEI (r=0.64), NNWI (~~25°N-40°N, 65°E-80°E) and southern peninsular India (SPI) (5°N-15°N, 75°E-80°E). Meanwhile, the hydrometeors' variability inside convective systems develop over these regions is considered to understand their association with LFR. The LFR values are low~~ r=0.42) and SPI (r=0.55). All the correlation values are strong and statistically significant at a 95% confidence level, indicating tight linearity in the relationship of LFD and graupel concentration over regions of higher lightning activity over India.

155 **3.2 Distribution of anomalous LFD during pre-monsoon season with respect to ENSO phases**

The LFD values are lower than the normal during the pre-monsoon season over NNWI when the ENSO phase is either warm or cold (Figure 3 (a, b)) ~~. However, the same region~~ and it exhibits an increase of ~~LFR~~ LFD during the neutral phase (Figure 3 (c)). While looking into the ~~LFR~~ LFD anomaly of individual years, pre-monsoons of three years (1997, 1998, and 2010) over NNWI have come under the El-Nino phase (Figure 4 (d)). The first two exhibits a decrease of ~~LFR over NNWI~~ LFD , contributing to

160 the overall reduction in the ~~LFR (figure 2~~ LFD over NNWI (Figure 3 (a)). Out of the four La-Nina years (1999, 2000, 2008, and 2011) of pre-monsoon season, 1999, 2000 and 2011 have below-average values of ~~LFR~~ LFD over the same region (Figure 4 (d)). ~~The pre-monsoons of 11 years occurred during the neutral phase of ENSO, in which six years are showing below and five years above-average values of LFR over NNWI.~~

~~Graupel and snow are the different forms of ice content inside the convective clouds.~~

165 In situ airborne observations during the Cloud-Aerosol Interaction and Precipitation Enhancement Experiment (CAIPEEX) over various locations of India shows that convective clouds during the pre-monsoon and monsoon period have an ice water content of 10^{-4} to 1 gm^{-3} (Patade et al., 2015). Moreover, in situ measured ice cloud properties in the European Cloud Radiation Experiment (EUCREX) have reported a similar range of ice water content inside the clouds system (10^{-4} gm^{-3} to 1 gm^{-3}) (Hogan et al., 2006). From TRMM observations and high-resolution model simulations, **?** reported ice concentrations of 10^{-3} to 10^{-2}

170 gm^{-3} for convective storms over the Indian region.

~~From figure 7 the anomalous latent heating exists mostly between +/- 0.01. In some cases, it is extending up to +/-0.02 (Kelvin/hr); additionaly, previous studies indicate these anomalous values are highly significant (Kumar et al., 2014). Linked with the decrease~~ The vertical profiles for graupel and snow concentration are shown over the hotspot domains of LFD in figures 5 and 6, respectively, revealing a significant disparity in their seasonal average with the observation region. These

175 figures clearly demonstrate that the seasonal average of graupel and snow ~~content over NNWI during the warm and cold phase of ENSO (Figures 5 (d), 6 (d)), latent heat (LH) release decreases (Figure 7 (d)). The anomalous negative SH at 300 hPa~~
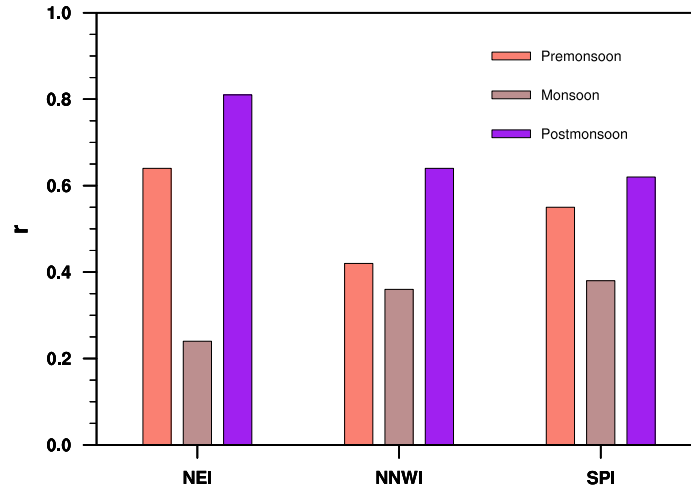
Figure 2. ~~Anomaly composite of LFR during different ENSO phases. The box in figure~~ Pearson correlation coefficient (~~d~~r) between LFD and ~~(g) indicates the region of monsoon trough~~ graupel concentration over NEI, NNWI and ~~western disturbance~~SPI during premonsoon, ~~respectively~~monsoon and post-monsoon season.

~~manifests that the clouds are unable to penetrate deep into the atmosphere during these two phases over NNWI (Figure 8 (a, b)) . As a result, LFR over NNWI in these phases is low, especially in the cold phase. Contrarily, higher LFR during the neutral phase pointing the abundance of graupel and snow inside the cloud system.~~

180 ~~It is noticed that ENSO warm phase during the pre-monsoon season is favourable to LFR over the NEI and SPIbut unfavourable to central India (CI) (Figure 3 (a)). Conversely, the cold ENSO phase suppresses LFR over NEI and SPI with enhanced LFR over CI (Figure 3 (b)). In short, the anomalous pattern of LFR during warm and cold phases are mirror images of each other during the pre-monsoon season . Most of the regions that exhibit an increase of LFR in the warm period show decreased LFR in the cold phase of ENSO. The entire years under the cold (warm) phase during pre-monsoon are showing a decrease (increase)~~

185 ~~of LFR over NEI (SPI) (Figure 4 (a, g)), which confirms that the cold phase suppresses the LFR over NEI, and the warm phase enhance it over SPI~~concentration are peaking around 6 Km over NEI, NNWI and SPI, and after that level, they shows a rapid decrease with height. Note that the seasonal average of latent heat (LH) over these hotspot domains of LFD are peaking between 6-7 Km range and dramatically coincides with the peaking altitude of graupel/snow concentration, mainly because of the release of energy during the phase transition of cloud droplets to ice particles (Figure 7). It is captivating that graupel/snow

190 concentrations are prominent during all three seasons over SPI, with a maximum value in the post-monsoon season. In contrast to this observation, the NEI and NNWI are showing a minimum value of graupel/snow concentrations during the post-monsoon season in India.

~~We display the vertical~~ The anomalous profile of graupel in figure 5 (a) ~~, which~~ indicates that clouds over NEI have high (low) graupel content during the ENSO warm (cold) phase. An increase of snow content with a peak value near 6.5 km is also
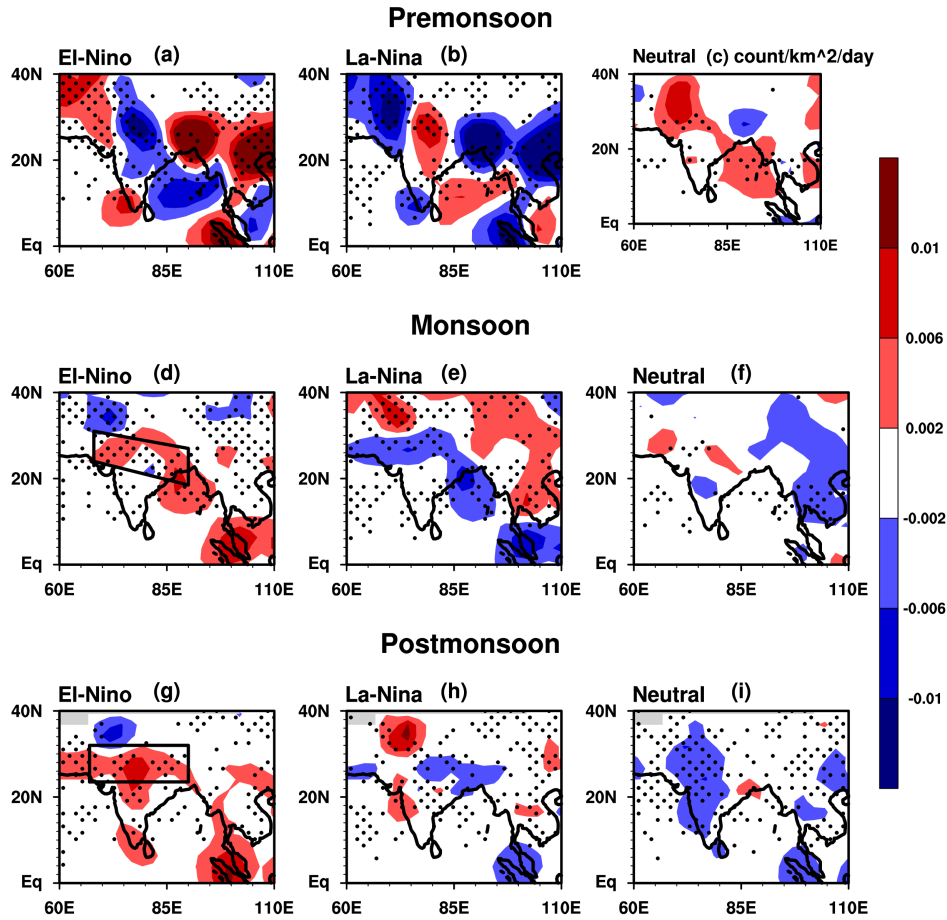
Figure 3. Anomaly composite of LFD during different ENSO phases with stippling indicates statistically significant areas at a 95% confidence level. The box in figure 3 (d) and (g) shows the monsoon trough and western disturbance region, respectively.

observed over NEI during pre-monsoon in the warm ENSO phase (Figure 6 (a)). The interaction between snow and graupel and the associated charge generation is responsible for ~~the occurrence of lightning in~~ lightning from convective clouds. Thus the formation of the higher ~~(lower)~~ amount of graupel and snow over NEI during the warm ~~(cold)~~ phase will release more latent heat, which is evident from figure 7 (a). Positive (negative) anomalies of SH over NEI indicates that the convective clouds formed during the ENSO warm (cold) phase are vigorous (wimpy) and consequently responsible for the enhanced (reduced) ~~LFR.~~ LFD. More importantly, graupel, snow, and latent heat profiles present below-average values in the neutral ENSO phase, which may confirm a decrease in lightning events over NEI.

From figure 7 the anomalous latent heating exists mostly between +/- 0.01. In some cases, it is extending up to +/-0.02 (Kelvin/hr); additionally, previous studies indicate these anomalous values are highly significant (Kumar et al., 2014). Linked with the decrease of graupel and snow content over NNWI during the warm and cold phase of ENSO (Figures 5 (~~g)and 6 (g)show that the~~ d), 6 (d)), LFD changes (Figure 7 (d)). The anomalous negative SH at 300 hPa manifests that the clouds are unable to penetrate deep into the atmosphere during these two phases over NNWI (Figure 8 (a, b)). As a result, LFD over NNWI in these phases is low, especially in the cold phase. Contrarily, higher LFD during the neutral phase pointing the abundance of graupel and snow inside the cloud system. It is noticed that ENSO cold phase during the pre-monsoon season is favourable to LFD over central India (CI) (Figure 3 (b)), and the converse is true for ENSO warm phase (Figure 3 (a)).

The graupel and snow concentrations over SPI are anomalously high up to 6 km during the cold phase of ENSO~~;~~, and above that level, it decreases (Figures 5,6 (d)) . This particular hydrometeor pattern reverses during the warm phase, exhibits below-average values beneath 6 km, and rapidly increases above that level. ~~Figure 7 (g) shows the level of maximum~~ A similar pattern is observed in the vertical profiles of latent heat release ~~follows the pattern of graupel and snow concentrations~~ above 6 km. Note that the analysis presented here confirms that the warm phase of ENSO intensifies the deep convection over SPI during the pre-monsoon season and hence promotes ~~LFR~~ LFD.

3.3 Distribution of anomalous ~~LFR~~ LFD during monsoon season with respect to ENSO phases

The ~~LFR~~ LFD over the monsoon trough region ~~and along the northwest coast~~ of India increases during the warm phase of ENSO (Figure 3 (d)) but it remarkably decreases during the cold phase (Figure 3 (e)). Based on the 1998-1999 El-Nino event, Hamid et al. (2001) suggested that intense convective storms developing over the maritime continents are responsible for the increase of lightning activity despite a decrease in the number of convective storms. During the El-Nino years of 1997-1998 and 2002-2003, the southeast Asian regime exhibited an above-average value of lightning (Kumar and Kamra, 2012). ~~An elongated region over central India is showing higher (lower) LFR during the warm (cold) phase of ENSO (Figure 3 (d, e)). While analysing~~ While analyzing the 300 hPa SH variability, we noticed that the amount of SH over ~~that region is high~~ the monsoon trough is higher during the warm and ~~low~~ lower during the cold phase (Figure 8 (d, e)). The NEI is showing a positive anomaly of ~~LFR during both warm and cold phases~~ LFD during the cold phase of ENSO. Figure 4 (b) enforces this result by showcasing that ~~all the years under the warm phase and the~~ majority of years under the cold phase (during the monsoon season) ~~show~~ shows an increase in ~~LFR~~ LFD over NEI. The ~~similarity of LFR anomaly over NEI during the warm and cold phaseis also noticeable in the~~ vertical profile of LH shows an above-average value during the cold phase, and this enhancement of LH in the mid-troposphere helps to increase atmospheric instability and deep convection. On the other hand, the vertical distribution of ~~graupel and snow displayed in figures~~ hydrometers are not displaying any compelling variability with ENSO phases over NEI (Figures 5 (b)~~and~~, 6 (b)~~. In contrast, LFR is enhanced (suppressed)~~). The observed increase (decrease) in the anomalous LFD over NNWI during the cold (warm) period ~~due to the presence of a larger (smaller) amount of graupeland snow~~ is captured well in the vertical profiles of graupel, snow and latent heat release (Figures 5 (e), 6 (e), 7 (e)) . There is no noticeable change in the distribution of ~~LFR~~ LFD over SPI in the three phases of ENSO (Figure 3 (d, e, f). ~~Further, anomalous LFR during the individual years are not showing any particular pattern corresponding to different ENSO phases over SPI (Figure 4 (h)).~~
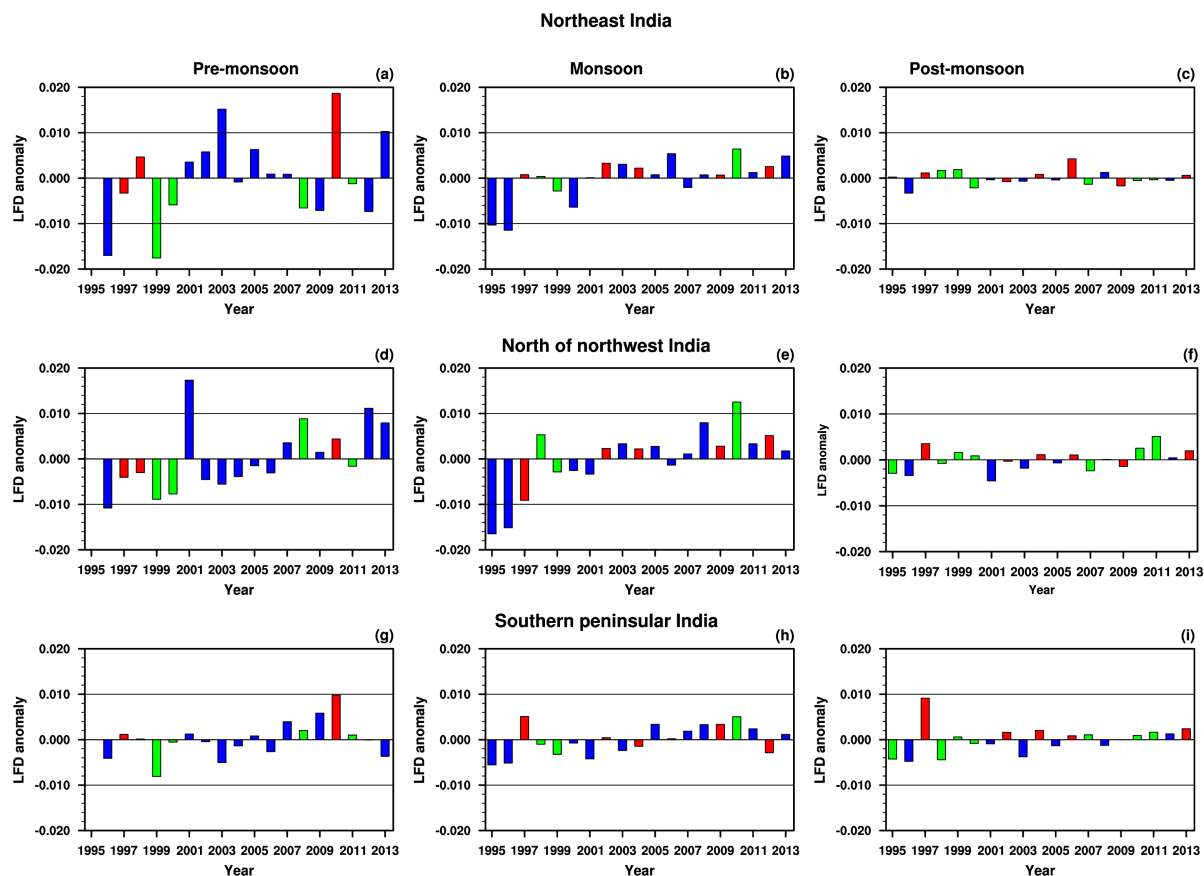
Figure 4. ~~The anomaly of LFR~~ Anomalous LFD during the individual years with different ENSO phases. ~~Red color~~ The red colour label bar corresponds to warm~~;~~ the green one corresponds to ~~the~~ cold, and the blue ~~color~~ colour label bar indicates the neutral phases of ENSO.

~~Composite anomaly of snow during different ENSO phases.~~
~~Composite anomaly of latent heat during different ENSO phases.~~
~~Anomaly composite of specific humidity at 300hPa during different ENSO phases.~~
~~Anomaly composite of geopotential height at 500hPa and 200hpa wind during different ENSO phases.~~

240   It is interesting to observe that during the 12 years from 2002 to 2013, 11 years have shown above-average values of ~~LFR~~ LFD over the NEI and NNWI regions (Figure 4 (b, e)), registering the intensification of deep convective cloud formation during the recent monsoon season over respective areas. Out of the nine years from 2005 to 2013, 8 have above-normal ~~LFR~~ LFD
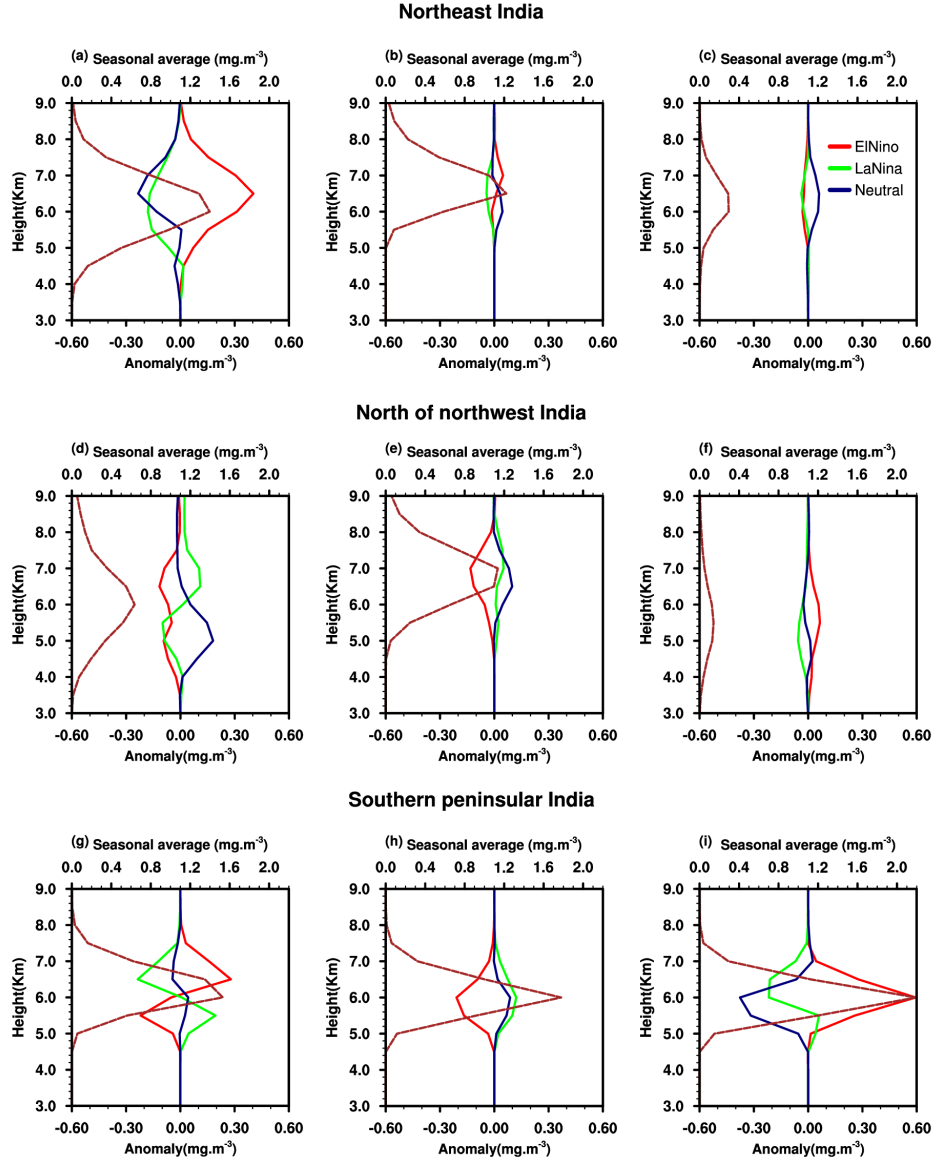
Figure 5. ~~Anomaly~~ Seasonal average (brown dotted curve) and anomaly composite of graupel concentration during different ENSO phases. (a, d, g): pre-monsoon season, (b, e, h): Monsoon season, (c, f, i): post-monsoon season.

over SPI (Figure 4 (h)). ~~This indicates~~ Thus indicating an escalation of deep convection over SPI in that period. Specifically, the hotspots of ~~LFR~~ LFD over the Indian land region became more prominent during the last decade's monsoon seasons.
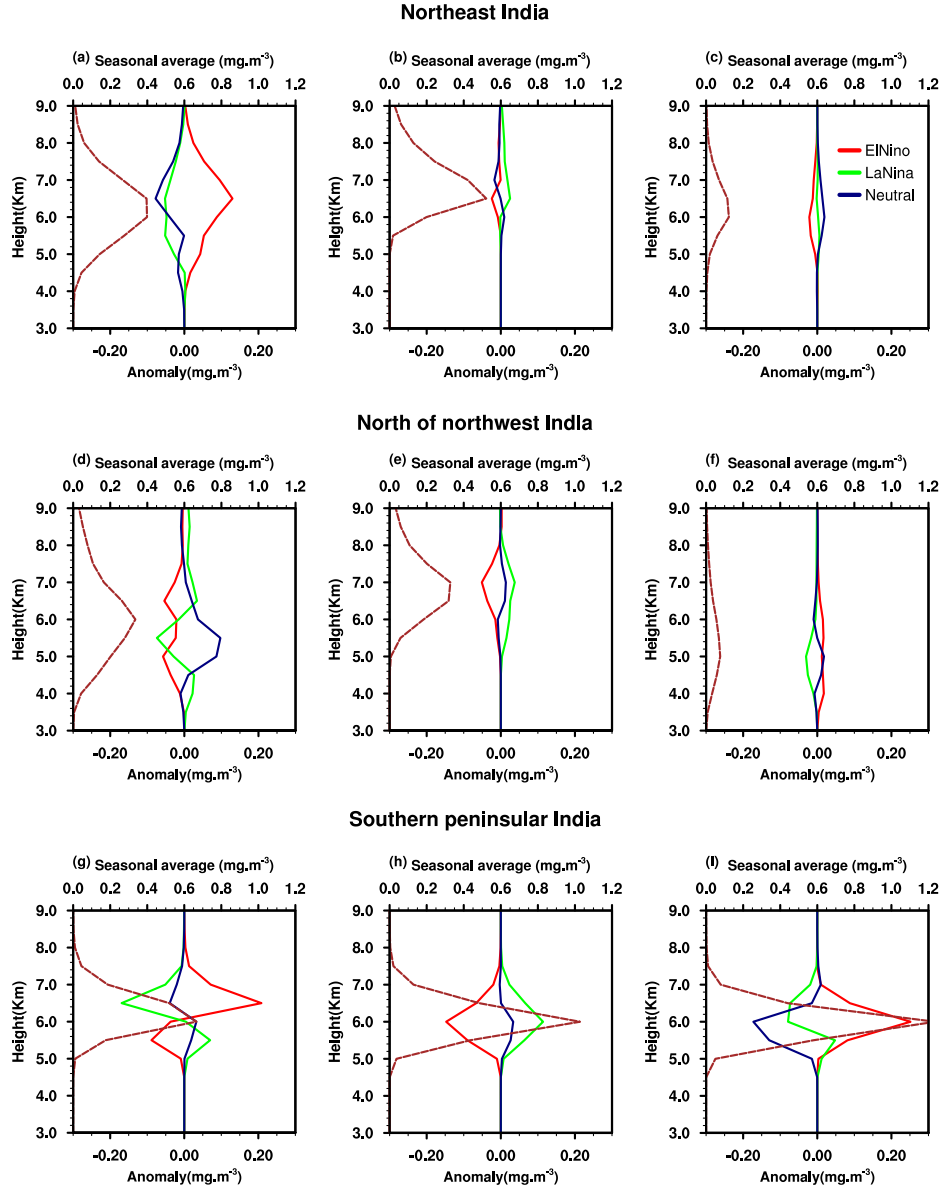
Figure 6. Seasonal average (brown dotted curve) and anomaly composite of snow concentration during different ENSO phases. (a, d, g): pre-monsoon season, (b, e, h): Monsoon season, (c, f, i): post-monsoon season.

245   **3.4   Distribution of anomalous ~~LFR~~ LFD during post-monsoon season with respect to ENSO phases**
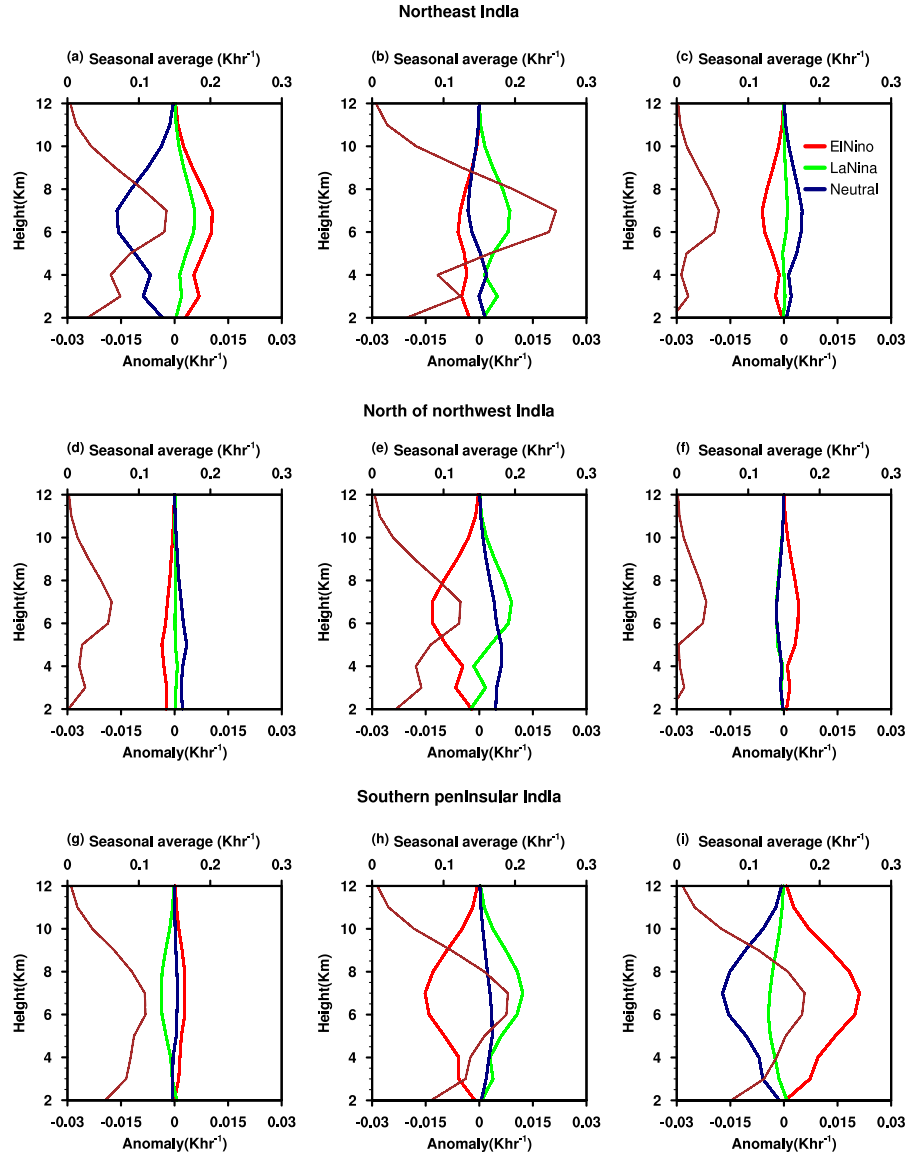
Figure 7. Seasonal average (brown dotted curve) and anomaly composite of latent heat during different ENSO phases. (a, d, g): pre-monsoon season, (b, e, h): Monsoon season, (c, f, i): post-monsoon season.

~~During the post-monsoon season,~~ Western disturbances (WD) ~~, which are~~ are the vertical perturbations associated with the subtropical westerly jet stream, ~~bring rainfall to India's northern regions~~ which is one of the potential contributors to the rainfall over northern India during the post-monsoon season (Dimri et al., 2016). The jet is more intense and propagates southward during the El-Nino phase of ENSO (Schiemann et al., 2009). Our analysis shows ~~during~~ at the time of the post-monsoon
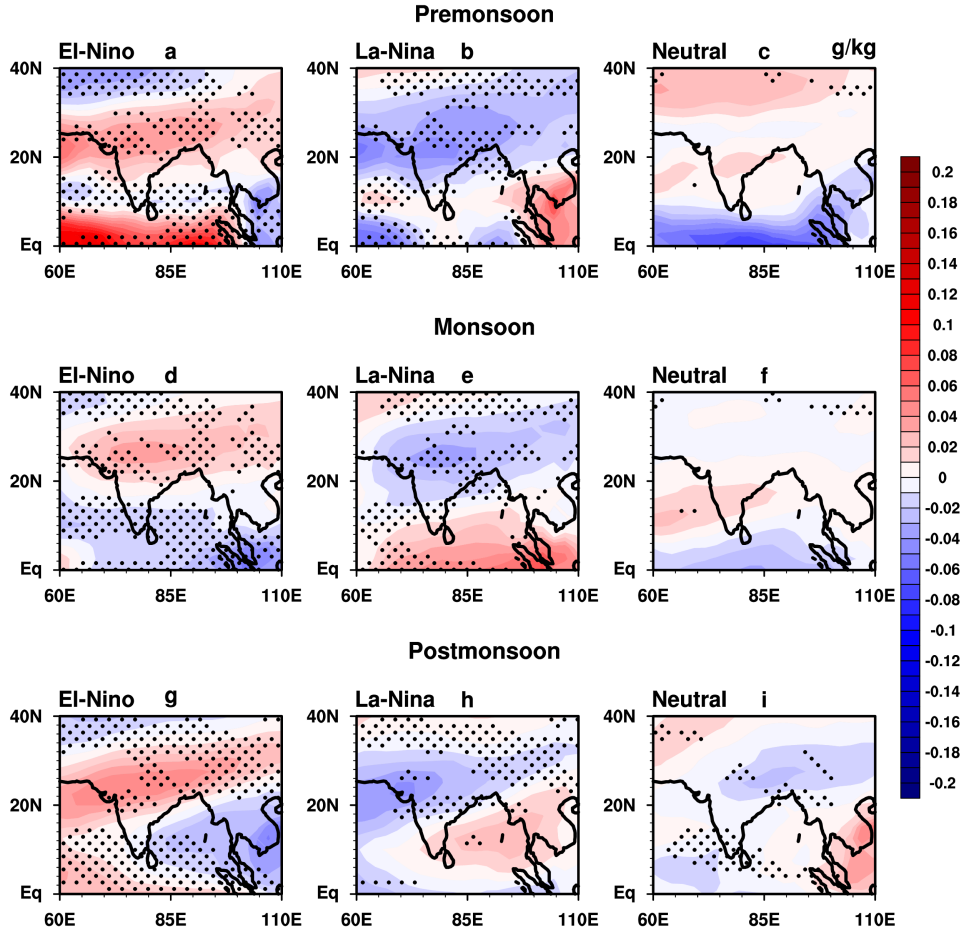
Figure 8. Anomaly composite of specific humidity at 300hPa during different ENSO phases with stippling to indicate statistically significant areas at a 95% confidence level.

250 El-Nino period, ~~LFR~~ LFD is increased throughout the country, and it is maximum over north-central India (Figure 3 (g)). In contrast, in the cold phase, intense ~~LFR~~ LFD is concentrated only over the NNWI (Figure 3 (h)). ~~Meanwhile, NEI and NNWI are not showing any significant difference in the vertical profile of snow and graupel with different ENSO phases during the post-monsoon season (Figures 5 (c, f) and 6 (c, f)).~~ Zubair and Ropelewski (2006) reported a significant role for ENSO in controlling the post-monsoon rainfall over SPI. The SPI is showing an increase of ~~LFR~~ LFD in the warm phase of ENSO

255 during this season due to the presence of clouds having higher graupel and snow content over that region (Figures 3 (g), 5 (i), 6 (i)). The entire years grouped under the warm phase of ENSO during the post-monsoon season show an increase of ~~LFR~~ LFD
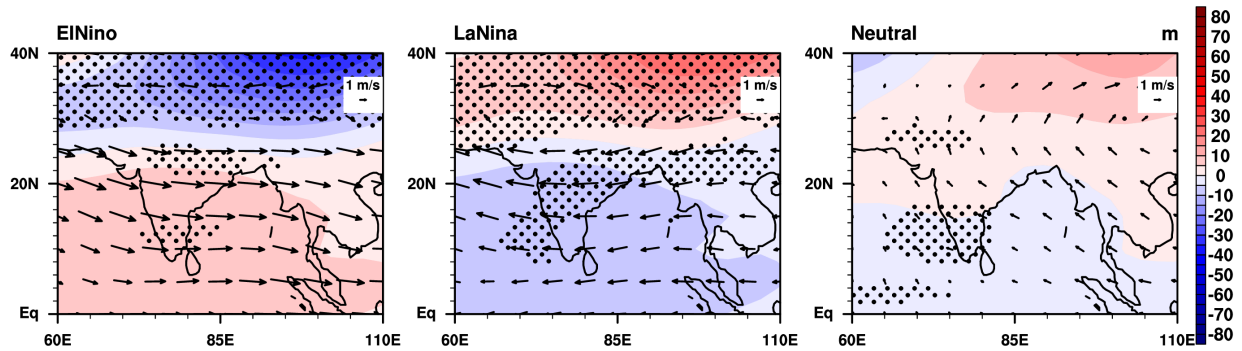
Figure 9. Anomaly composite of geopotential height at 500hPa and 200hPa wind during different ENSO phases. The stippling indicates statistically significant areas of geopotential height at a 95% confidence level.

over SPI. On the other hand, during the cold phase, anomalous ~~LFR~~ LFD displays an inconsistent pattern of oscillation (Figure 4 (i)).

Climate variability, like ENSO, can alter the position of jet streams and hence the distribution of WD (Hunt et al., 2018). Syed et al. (2006) identified that the intensification of WDs during the El-Nino is associated with the weakening of Siberian high. Studies signify that depressions formed over the South Bay of Bengal and the Arabian Sea can also modulate WDs' path (Rao et al., 1969). ~~It is exciting to note that~~ The 500 hPa GP surface ~~drops-down~~ drops down (go up) ~~from the~~ beyond 25°N ~~towards the north~~ latitude and indicates the ~~suppression~~ reduction (enhancement) of convection over that region during the warm (cold) phase of ENSO (Figure 9 (a, b)). ~~In contrast~~Meanwhile, a higher (lower) GP surface is visible all over India during the warm (cold) phase, which is an indication of an increase (decrease) in the convective activity during the respective phases. By considering the anomalous circulation at 200 hPa level, an anomalous westerly (easterly) wind is prevalent over entire India during warm (cold) periods (Figure 9~~(a, b)~~). Accordingly, upper-level wind pattern and variability of GPH together indicate the southward extension of WD during ENSO's warm phase. The sharp increase (decrease) of SH lies precisely over the region of the maximum undulation of GPH over India during the warm (cold) phase (Figure 8 (g, h)). This suggests that ENSO indirectly influences the ~~LFR~~ LFD over India during the post-monsoon season by modulating WDs' path.

4 Conclusion

In this study, we have discussed the influence of ENSO on ~~LFR during pre-monsoon~~LFD distribution during premonsoon, monsoon, and post-monsoon seasons over India. Regardless of ENSO phases, the ~~LFR~~ LFD is peaking at the time of pre-monsoon season over NEI and SPI. However, the NNWI exhibits a peak ~~LFR~~ LFD during the monsoon season. ~~The LFR~~

275 More importantly, the compelling correlation values indicates the solid linear dependence of LFD on graupel concentration over the hotspot regions of lightning. The LFD is increased (decreased) compared to their average values over NEI and SPI during the warm (cold) phase of ENSO, and anomalies of the charge generating hydrometeors ~~show~~ are also showing a similar kind of swing ~~. Furthermore, the entire years under the cold (warm) phase~~ during the pre-monsoon season~~taken in this study is characterized by a decrease (increase) of LFR over NEI (SPI), which firmly indicates that the cold phase suppresses the LFR~~

280 ~~over NEI, and the warm phase enhance it over SPI.~~

~~During the cold phase in pre-monsoon, graupel and snow concentration over SPI shows an above-average value up to 6 km. This particular pattern of these hydrometeors reverses during the warm phase. The~~ . An increase in graupel and snow formation above 6 km pinpoint that the warm phase of ENSO is conducive for deep convection over SPI during the pre-monsoon ~~and hence higher LFR~~season. However, the neutral phase of ENSO favours the deepening of clouds over NNWI, as evidenced by

285 the high values of the upper level-specific humidity. ~~At the time of~~

~~During~~ monsoon season, ~~LFR over NEI is high during both El-Nino and La-Nina periods. Over NNWI , LFR increases during~~ LFD over NEI and NNWI is higher than the average values during the La-Nina ~~but diminishes during El-Nino~~periods. The SPI ~~does not show~~ is not showing significant variation in ~~LFR~~ LFD with respect to different ENSO phases during the monsoon season. While considering the recent 12 years of this study, irrespective of the ENSO phases, every year has displayed

290 above-average values of ~~LFR~~ LFD over the NEI and NNWI region. Out of 9 years from 2005 to 2013, 8 displayed above-normal ~~LFR~~ LFD over SPI, which signifies the intensification of ~~LFR~~ LFD over the three hotspots ~~in the last decades of the monsoon season.~~ during the monsoon seasons of the last decade.

Almost all regions in India are exhibiting higher ~~LFR~~ LFD during the warm ENSO phase in the post-monsoon season. The elevated (reduced) GPH is visible all over India during the warm (cold) phase of ENSO, which is an indication of an increase

295 (decrease) in the convective activity during the respective phases. Further, the intensification of convection during the warm phase is advocated by a significant rise of graupel and snow concentration over SPI. The entire years grouped under the warm phase of ENSO during the post-monsoon season show an increase of ~~LFR~~ LFD over SPI, whereas the years elected under the cold phase shows a disperse anomalous pattern. Both intensification and southward extension of WD is responsible for higher ~~LFR~~ LFD over India in the warm phase, indicating indirect interaction between ENSO and ~~LFR~~ LFD by modulating

300 the mid-latitude westerlies.

Data availability. The LIS/OTD data and vertical profiles of hydrometeors, and latent heat obtained from the website http://ghrc.nsstc.nasa.gov/ and https://disc.gsfc.nasa.gov/datasets/ respectively. The GPH, wind and SH data are avilable the weblink https://psl.noaa.gov/data/gridded/ data.ncep.reanalysis.html. The HadISST data used in this work is accessible from the weblink https://psl.noaa.gov/gcos$_w$gsp/.

Author contributions. The paper and its methodology were conceptualized and developed by SA, AVS, and PV; AVS performed the analyses, and PV curated the data. The original draft preparation was by AVS; further reviewing and editing was by PV and SA. AVS handled visualization.

Competing interests. The authors declare that they have no known competing financial interests or personal relationships that could have appeared to influence the work reported in this paper.

Acknowledgements. We are grateful to NASA and PSL for providing LIS/ODT, TRMM, and NCEP Reanalysis data products, respectively, which are used in this study. Sreenath A V acknowledges Kerala State Council for Science, Technology, and Environment (KSCSTE), India, for providing financial support. Support from the Department of Atmospheric Sciences, Cochin University of Science and Technology is acknowledged.

305

310 References

Ahmad, A. and Ghosh, M.: Variability of lightning activity over India on ENSO time scales, Advances in Space Research, 60, 2379–2388, 2017.

Blakeslee, R. J., Mach, D. M., Bateman, M. G., and Bailey, J. C.: Seasonal variations in the lightning diurnal cycle and implications for the global electric circuit, Atmospheric research, 135, 228–243, 2014.

315 Cecil, D. J., Buechler, D. E., and Blakeslee, R. J.: Gridded lightning climatology from TRMM-LIS and OTD: Dataset description, Atmospheric Research, 135, 404–414, 2014.

Cess, R. D., Zhang, M., Wielicki, B. A., Young, D. F., Zhou, X.-L., and Nikitenko, Y.: The influence of the 1998 El Niño upon cloud-radiative forcing over the Pacific warm pool, Journal of climate, 14, 2129–2137, 2001.

Christian, H. J., Blakeslee, R. J., Boccippio, D. J., Boeck, W. L., Buechler, D. E., Driscoll, K. T., Goodman, S. J., Hall, J. M., Koshak, W. J., 320 Mach, D. M., et al.: Global frequency and distribution of lightning as observed from space by the Optical Transient Detector, Journal of Geophysical Research: Atmospheres, 108, ACL–4, 2003.

Chronis, T., Goodman, S., Cecil, D., Buechler, D., Robertson, F., Pittman, J., and Blakeslee, R.: Global lightning activity from the ENSO perspective, Geophysical Research Letters, 35, 2008.

Cooray, V., Rakov, V., and Theethayi, N.: The lightning striking distance—Revisited, Journal of Electrostatics, 65, 296–306, 2007.

325 Dimri, A., Yasunari, T., Kotlia, B., Mohanty, U., and Sikka, D.: Indian winter monsoon: Present and past, Earth-science reviews, 163, 297–322, 2016.

Goodman, S., Buechler, D., Knupp, K., Driscoll, K., and McCaul Jr, E.: The 1997–98 El Nino event and related wintertime lightning variations in the southeastern United States, Geophysical Research Letters, 27, 541–544, 2000.

Goodman, S., Buechler, D., and McCaul, E.: Lightning, in Our Changing Planet: The View From Space, 44–52, 2007.

330 Goswami, B. B., Mukhopadhyay, P., Mahanta, R., and Goswami, B.: Multiscale interaction with topography and extreme rainfall events in the northeast Indian region, Journal of Geophysical Research: Atmospheres, 115, 2010.

Hamid, E. Y., Kawasaki, Z.-I., and Mardiana, R.: Impact of the 1997–98 El Niño event on lightning activity over Indonesia, Geophysical Research Letters, 28, 147–150, 2001.

Hogan, R. J., Mittermaier, M. P., and Illingworth, A. J.: The retrieval of ice water content from radar reflectivity factor and temperature and 335 its use in evaluating a mesoscale model, Journal of Applied Meteorology and Climatology, 45, 301–317, 2006.

Houze Jr, R. A., Wilton, D. C., and Smull, B. F.: Monsoon convection in the Himalayan region as seen by the TRMM Precipitation Radar, Quarterly Journal of the Royal Meteorological Society: A journal of the atmospheric sciences, applied meteorology and physical oceanography, 133, 1389–1411, 2007.

Hsu, C.-P. F. and Wallace, J. M.: The global distribution of the annual and semiannual cycles in precipitation, Monthly Weather Review, 104, 340 1093–1101, 1976.

Hunt, K. M., Turner, A. G., and Shaffrey, L. C.: The evolution, seasonality and impacts of western disturbances, Quarterly Journal of the Royal Meteorological Society, 144, 278–290, 2018.

Kamra, A. and Athira, U.: Evolution of the impacts of the 2009–10 El Niño and the 2010–11 La Niña on flash rate in wet and dry environments in the Himalayan range, Atmospheric Research, 182, 189–199, 2016.

345 Kandalgaonkar, S., Kulkarni, J., Tinmaker, M., and Kulkarni, M.: Land-ocean contrasts in lightning activity over the Indian region, International Journal of Climatology: A Journal of the Royal Meteorological Society, 30, 137–145, 2010.

Kent, G., Williams, E., Wang, P., McCormick, M., and Skeens, K.: Surface temperature related variations in tropical cirrus cloud as measured by SAGE II, Journal of Climate, 8, 2577–2594, 1995.

Kilinc, M. and Beringer, J.: The spatial and temporal distribution of lightning strikes and their relationship with vegetation type, elevation,
350   and fire scars in the Northern Territory, Journal of climate, 20, 1161–1173, 2007.

Kulkarni, M. and Siingh, D.: The relation between lightning and cosmic rays during ENSO with and without IOD—a statistical study, Atmospheric Research, 143, 129–141, 2014.

Kumar, P. R. and Kamra, A.: Variability of lightning activity in South/Southeast Asia during 1997–98 and 2002–03 El Nino/La Nina events, Atmospheric research, 118, 84–102, 2012.

355 Kumar, S., Hazra, A., and Goswami, B.: Role of interaction between dynamics, thermodynamics and cloud microphysics on summer monsoon precipitating clouds over the Myanmar Coast and the Western Ghats, Climate dynamics, 43, 911–924, 2014.

Lau, K.-M., Ramanathan, V., Wu, G.-X., Li, Z., Tsay, S., Hsu, C., Sikka, R., Holben, B., Lu, D., Tartari, G., et al.: The Joint Aerosol–Monsoon Experiment: A new challenge for monsoon climate research, Bulletin of the American Meteorological Society, 89, 369–384, 2008.

Mills, B., Unrau, D., Pentelow, L., and Spring, K.: Assessment of lightning-related damage and disruption in Canada, Natural hazards, 52,
360   481–499, 2010.

Murugavel, P., Pawar, S., and Gopalakrishan, V.: Climatology of lightning over Indian region and its relationship with convective available potential energy, International Journal of Climatology, 34, 3179–3187, 2014.

Patade, S., Prabha, T., Axisa, D., Gayatri, K., and Heymsfield, A.: Particle size distribution properties in mixed-phase monsoon clouds from in situ measurements during CAIPEEX, Journal of Geophysical Research: Atmospheres, 120, 2015.

365 Petersen, W. A., Rutledge, S. A., and Orville, R. E.: Cloud-to-ground lightning observations from TOGA COARE: Selected results and lightning location algorithms, Monthly weather review, 124, 602–620, 1996.

Rao, Y., Srinivasan, V., Raman, S., and RAMAKRISHNAN, A.: Forecasting manual, Part-II, Discussion of typical synoptic weather situation, winter-western disturbances and their associated features. FMU Report No. III-1.1, India Meteorological Department. Delhi, India, 1969.

Rasmussen, K. L. and Houze Jr, R. A.: Orogenic convection in subtropical South America as seen by the TRMM satellite, Monthly Weather
370   Review, 139, 2399–2420, 2011.

Romatschke, U., Medina, S., and Houze Jr, R. A.: Regional, seasonal, and diurnal variations of extreme convection in the South Asian region, Journal of climate, 23, 419–439, 2010.

Rosenfeld, D.: TRMM observed first direct evidence of smoke from forest fires inhibiting rainfall, Geophysical research letters, 26, 3105–3108, 1999.

375 Sátori, G., Williams, E., and Lemperger, I.: Variability of global lightning activity on the ENSO time scale, Atmospheric Research, 91, 500–507, 2009.

Schiemann, R., Lüthi, D., and Schär, C.: Seasonality and interannual variability of the westerly jet in the Tibetan Plateau region, Journal of Climate, 22, 2940–2957, 2009.

Selvi, S. and Rajapandian, S.: Analysis of lightning hazards in India, International Journal of Disaster Risk Reduction, 19, 22–24, 2016.

380 Singh, O. and Singh, J.: Lightning fatalities over India: 1979–2011, Meteorological Applications, 22, 770–778, 2015.

Syed, F., Giorgi, F., Pal, J., and King, M.: Effect of remote forcings on the winter precipitation of central southwest Asia part 1: observations, Theoretical and Applied Climatology, 86, 147–160, 2006.

Takahashi, T., Tajiri, T., and Sonoi, Y.: Charges on graupel and snow crystals and the electrical structure of winter thunderstorms, Journal of the atmospheric sciences, 56, 1561–1578, 1999.

385 Tinmaker, M., Aslam, M., and Chate, D.: Lightning activity and its association with rainfall and convective available potential energy over Maharashtra, India, Natural Hazards, 77, 293–304, 2015.

Venevsky, S.: Importance of aerosols for annual lightning production at global scale., Atmospheric Chemistry & Physics, 14, 2014.

Williams, E., Rosenfeld, D., Madden, N., Gerlach, J., Gears, N., Atkinson, L., Dunnemann, N., Frostrom, G., Antonio, M., Biazon, B., et al.: Contrasting convective regimes over the Amazon: Implications for cloud electrification, Journal of Geophysical Research: Atmospheres,
390 107, LBA–50, 2002.

Williams, E. R.: The Schumann resonance: A global tropical thermometer, Science, 256, 1184–1187, 1992.

Williams, E. R.: The electrification of severe storms, in: Severe Convective Storms, pp. 527–561, Springer, 2001.

Williams, E. R., Geotis, S., Renno, N., Rutledge, S., Rasmussen, E., and Rickenbach, T.: A radar and electrical study of tropical "hot towers", Journal of the atmospheric sciences, 49, 1386–1395, 1992.

395 Yadava, P. K., Soni, M., Verma, S., Kumar, H., Sharma, A., and Payra, S.: The major lightning regions and associated casualties over India, Natural Hazards, 101, 217–229, 2020.

Yang, S., Lau, K., and Kim, K.: Variations of the East Asian jet stream and Asian–Pacific–American winter climate anomalies, Journal of Climate, 15, 306–325, 2002.

Zipser, E. J.: Deep cumulonimbus cloud systems in the tropics with and without lightning, Monthly weather review, 122, 1837–1851, 1994.

400 Zipser, E. J., Cecil, D. J., Liu, C., Nesbitt, S. W., and Yorty, D. P.: Where are the most intense thunderstorms on Earth?, Bulletin of the American Meteorological Society, 87, 1057–1072, 2006.

Zubair, L. and Ropelewski, C. F.: The strengthening relationship between ENSO and northeast monsoon rainfall over Sri Lanka and southern India, Journal of Climate, 19, 1567–1575, 2006.